SEARCH FOR COMETARY ACTIVITY IN KBO (24952) 1997 QJ_4

K. J. MEECH and O. R. HAINAUT
Institute for Astronomy, University of Hawaii; European Southern Observatory

H. BOEHNHARDT and A. DELSANTI
MPI-Heidelberg; Obs. Paris, Meudon

Abstract. Deep imaging was performed with the Subaru Telescope on Mauna Kea centered on the position of the KBO (24952) 1997 QJ_4 on 2 half-nights during October 2002. A deep search for evidence of a dust coma was conducted which could be indicative of cometary activity down to a limit of $m_V = 31$ mag arcsec^{-2}. No coma was detected, and from this sensitive upper limits on dust production can be set at $Q < 0.01$ kg s^{-1}. Brightness variations consistent with rotational modulation were seen, implying a period of rotation longer than 4 hrs, with a range > 0.3 mag corresponding to a minimum projected axis ratio of 1:1.3.

1. Background

Kuiper belt objects display a range of surface colors from neutral (solar) to very red (see Figure 1). Near-IR spectroscopy of a handful of KBOs has revealed water-ice absorption features on a few, possibly organics and amorphous carbon, and many which are featureless (see Table I). This diversity is likely to be the result of several processes. One possibility is a competition between a reddening of the surface by high energy particles and collisions which can excavate more neutral material (Jewitt and Luu, 2001; Stern, 2001; Gil-Hutton, 2002). However, statistical work on the color distributions lead to contradictions with this model. For instance, the dispersion of colors over all the objects is much larger than the dispersion of colors for any given object (over rotational phase), suggesting that the bodies have uniform colors, while the collision/reddening model predicts variegated surfaces (Hainaut and Delsanti, 2002). Another suggestion, based on the observation of a color trend with inclination (Trujillo and Brown, 2002), is that the high inclination objects form a "hot" population of objects which were scattered during planet migration (Gomes, 2003) from smaller heliocentric distances. In this scenario, the color diversity might simply reflect different source regions.

There is another intriguing explanation for the diversity suggested from observations of (19308) 1996 TO_{66}, which is one of the bluest KBOs. The light curve of this object was seen to change dramatically from one year to the next. Complex rotation and collisions were discarded, but cometary activity is compatible with the strange change in its lightcurve (Hainaut et al., 2000). In this scenario, activity caused a change in surface albedo by removing some of the older, reddened

Earth, Moon and Planets **92:** 169–181, 2003.

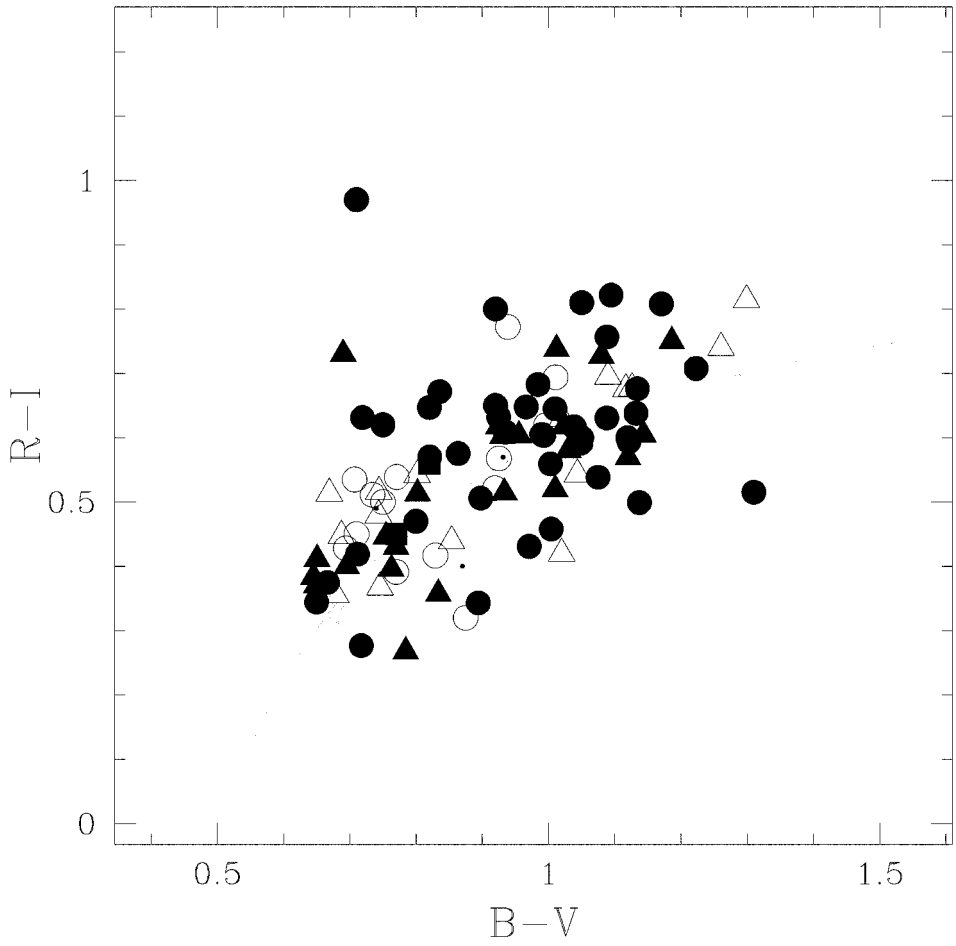

Figure 1. Color-color plot from (Hainaut and Delsanti, 2002) showing the large TNO color diversity. The star shows the solar color. The thin line is the locus of objects which display a linear reflectivity spectrum.

surface, and replacing it with bluer material. This hypothesis was strengthened by additional observations of (19308) 1996 TO_{66} after the change in light curve which showed that the object had become bluer and there was a variation in color over rotational phase (Sekiguchi et al., 2002). There has been reported activity now in 5 Centaurs:⋆ C/2000 T_4, 2060 Chiron, C/2000 B_4, C/2001 M_{10}, and more recently (29981) 1999 TD_{10} (Choi et al., 2003), which like Chiron is relatively blue. However, there has been no direct evidence of activity in any KBO to date.

⋆ There are several definitions of Centaur membership; some include known comets such as 39P/Oterma, 29P/Schwassmann-Wachmann 1, and C/2001 T4 (NEAT). This latter object exhibits cometary activity but is formally classified as a Centaur and has a very Chiron-like orbit (Bauer et al., 2003) with well-observed activity.

TABLE I
KBO surface composition and color

KBO[a]		$m_V - m_R$[b]	Spectral Features	Ref[c]
(15789)	1993 SC	0.54–0.70	hydrocarbons? featureless	1, 2
(26181)	1996 GQ_{21}	0.72	flat, Titan tholin, H_2O, C	3,4,5
(15874)	1996 TL_{66}	0.34–0.63	featureless	6
(19308)	1996 TO_{66}	0.26–0.48	strong H_2O	7
	1996 TS_{66}	0.43–0.76	featureless	2
(47171)	1999 TC_{36}	0.68–0.73	Titan tholin, amorph C, H_2O	8
(26375)	1999 DE_9	0.58	H_2O, organics, C	2,3,4
(38628)	2000 EB_{173}	0.55	featureless, H_2O?	2,9,10
(20000)	2000 WR_{106}	0.71	H_2O?	9
	2001 BL_{41}		Titan tholin, ice, C	5
(28978)	2001 KX_{76}		featureless	11,12

[a](38628) 2000 EB_{173} = Huya; (20000) 2000 WR_{106} = Varuna; (28978) 2001 KX_{76} = Ixion.
[b]Colors from (Delsanti et al., 2001; Boehnhardt et al., 2001; Hainaut and Delsanti, 2002).
[c]References cited: 1 – (Brown et al., 1997); 2 – (Jewitt and Luu, 2001); 3 – (Doressoundriam et al., 2003); 4 – (Boehnhardt et al., 2002); 5 – KBO ESO Large Program, presented at KBO meeting, in this volume, 2003; 6 – (Luu and Jewitt, 1998); 7 – (Brown et al., 1999); 8 – (Dotto et al., 2003); 9 – (Licandro et al., 2001); 10–(Brown et al., 2000); 11 – (Licandro et al., 2002); 12 – (Doressoundiram et al., 2002).

The Centaur Chiron has had possible detections of CO outgassing (Womack and Stern, 1999), and CN (Bus et al., 1991), and water-ice absorption features (Luu et al., 2000) have been seen in its near-IR spectrum. Modelling Chiron's activity shows that all the observations are consistent with H_2O-ice annealing (Prialnik et al., 1995). Prialnik's evolutionary thermal models, however, predict that for large bodies (e.g., $R_N >> 100$ km) energy from radioactive decay of ^{26}Al can create a low-porosity layer depleted in volatiles some 10–15 km below the surface and that much of the body will have been heated. Other cases of activity in distant minor bodies have been reported, such as an outburst of 1P/Halley at 14 AU (West et al., 1991), or continued activity in C/1995 O1 (Hale-Bopp) at 17 AU (Hainaut, personal communication) and a large number of dynamically new comets (Meech, 1999).

Equilibrium surface temperatures in the Kuiper belt are in the range of 40-60K. Only the more volatile species have sublimation temperatures in this range: (CO–25K, N_2–22K, CH_4–31K), however, amorphous H_2O-ice anneals at 35K and can release volatiles. The only realistic way to get much activity at the large distances for objects in the Kuiper belt is from sublimation of highly volatile materials. However, the low temperature laboratory ice experiments suggest that there should not be a large amount of this material available for sublimation since most of it should

be trapped in the condensed water-ice. For a detailed discussion of the activity mechanisms at large distances, see (Meech and Svoreň, 2004).

1.1. DETECTION OF ACTIVITY

The faint coma of Chiron, which was just visible in the discovery images (r = 11.8 AU; (Meech and Belton, 1990)); had a surface brightness of 22 mag arcsec^{-2} 2″ from the center, and was detected out to 8″ at 26 mag arcsec^{-2}. Much deeper observations under conditions of good seeing should yield higher S/N limits at least 2–3 mag fainter than this. At the distances of the KBOs, the gas ejection velocity from sublimation of CO is near 0.1 km s^{-1}, which would drag dust from the nucleus. Mass losses of a few $\times$ 0.01 kg s^{-1} would be detectable. This assumes that the coma is populated by tiny grains at the critical upper limit mass threshold for lift-off, $a_g = 0.1$ μm for the gas sublimation velocities expected at this distance. This is the equivalent of a total mass loss of 0.09 kg s^{-1}, or about 10^{24-25} molec s^{-1}.

The CO outgassing sporadically detected in Chiron (although some of these observations are controversial) was at levels of 1.5 $\times$ 10^{28} molec s^{-1} near 12 AU. Comet C/1995 O1 (Hale–Bopp) was outgassing at a rate of 10^{28} molec s^{-1} at r = 9 AU, and scaling the production as $Q_{CO} \propto r^{-2} \times D^2$, where D is the object diameter, suggests that something as active as Hale Bopp should have CO outgassing at a rate of 10^{27} molec s^{-1} at a distance of r = 35 AU. Bockelée-Morvan et al. (2001) placed upper limits between 0.7–10 $\times 10^{28}$ molec s^{-1} from sub-mm observations of several KBOs. The outgassing limits which can be placed using low surface brightness detection of dust coma are much more stringent than the current limits on KBO activity, so that even a negative result would be highly significant.

1.2. PENCIL BEAM SURVEY

Currently, there is a sharp cut off in mass near r = 47 AU, the reasons for this deficiency are still being investigated (Brunini and Melita, 2002; Kobayashi and Ida, 2001; Weidenschilling, 2003). Until recently, that distance corresponded uncomfortably to the limiting magnitude ($\sim$ 25) of the TNO surveys. However, several recent deep "pencil-beam" surveys are pushing the limits to 1–2 mag fainter, with an area sufficient so that many objects should have been detected. It is now clear that a change of regime happens at this distance. It can either be that (i) there are no TNOs beyond that limit (e.g., because the proto-planetary nebula has been truncated, or (ii) because the most distant TNOs are on a different regime that caused their accretion and evolution to be different. Beyond the 2:1 Neptune resonance at 47 AU, the gravitational influence of the planets becomes negligible. As a consequence, the orbits of the planetesimals remain un-perturbed, and they will form a dynamically "cold" disk, populated by very small objects. Their accretion process will be dominated by low velocity collisions, leading to very thin disk,

whose thickness is directly related to the median size of the objects, which in turn is related to the density of that region. Current estimates of that thickness put it in the 0.5–2° range (Hahn, 2000). Unfortunately, most pencil-beam surveys were aimed directly at the ecliptic. If the cold disk is inclined to the ecliptic by as little as 1–2° (e.g., if it is located in the barycentric plane of the Solar System), it has simply been missed. In the process of taking a series of images to do a very deep imaging search for dust around a Kuiper belt object, data are collected which are suitable for an extremely deep pencil beam survey (Kinoshita et al., 2004).

Table II lists a subset of KBOs with blue-neutral colors compared to the Sun (m_V–m_R = 0.36). The optimum candidate would be one with blue colors, at small r (to maximize coma detectability), and which would be near the invariable plane. The first choice of an object because of color was (24952) 1997 QJ_4, and the targets which are close to the barycentric plane included 1997 RT_5 and 2000 PE_{30}.

2. Observations

The observations were obtained on the first half of the nights of 2002 October 3 and 4 UT using the Subaru 8-m telescope with Suprime-Cam (Miyazaki et al., 1998). Suprime-Cam is a mosaic of ten 2048×2048 CCDs. The camera has a plate scale of 0.2″ pixel^{-1} which yields a field of view of 34′×27′. The detector gain is 2.5 e^-/ADU, and the read noise 10 e^-. Because superb flattening is required in order to search for very low surface brightness coma, the images were accumulated in 400 sec exposures, dithering the telescope between each exposure. (24952) 1997 QJ_4 was centered in the best part of the most sensitive chip as the starting point of the dither, and offsets were chosen to keep the KBO on this chip. The images were all guided at sidereal rates. The exposure time (400s) was selected to ensure that any trailing due to the motion of the KBO was within the seeing disk, which was stable between 0.6–0.7″ on both nights.

On the first night, 31 images were taken under photometric conditions, but there was thick cirrus present off and on during night 2, and only 16 images were obtained. Seven standard stars (Landolt, 1992) with a range of m_V–m_R colors from −0.092 to 1.066 were observed on night 1 to compute extinction (k_V = 0.109±0.001 mag airmass^{-1}) and calibrate to absolute fluxes.

3. Analysis

Both twilight sky flats and dome flats were obtained for these images and used for the initial flattening. In addition, dark sky flats were made by median combining the images themselves (excluding extended galaxies) in order to apply a second order correction. In this manner the resulting images are “super-flattened” to a level that is better than 0.1% across the chip, and much better than this in the vicinity of the KBO. A single image from night 1 is shown in Figure 2a.

TABLE II
KBO candidates for activity

Obj	V–R	Cls	α^a	δ^a	m_V	λ^b	ϕ^b	r[AU]
1997 QJ_4 (24952)	0.296	Plut	00:05	+06:35	23.0	5.43	5.4 .	33.83
1999 RY_{215}	0.358	QB1	22:03	−09:58	22.9	331.02	1.8	36.70
1999 OY_3	0.358	QB1	20:31	−16:19	22.9	307.41	2.5	39.30
1996 TO_{66} (19308)	0.377[c]	QB1	00:05	+05:54	21.3	4.67	4.8 .	46.22
2000 CG_{105}	0.390	QB1	09:19	+14:16	23.3	136.50	−1.3	46.55
1995 SM_{55} (26308)	0.394	QB1	01:48	+17:21	20.8	32.36	5.7 .	29.21
2000 CL_{105}	0.410	QB1	09:27	+16:48	22.7	137.71	1.7	45.02
1998 SN_{165} (35671)	0.446	QB1	23:47	−00:11	21.8	358.41	1.1 .	38.05
1997 RT_5	0.474	QB1	23:22	−05:41	23.7	350.43	−1.5	42.33
1999 RJ_{215}	0.302	Scat	22:53	+05:02	23.0	348.28	11.1	34.78
1996 TL_{66} (15874)	0.334	Scat	02:50	+12:59	20.9	44.93	−3.1 .	35.05
2000 PE_{30}	0.380	Scat	20:36	−18:47	22.1	307.80	−0.2	37.27
2000 CQ_{105}	0.390	Scat	09:31	+17:37	23.0	138.40	2.7	49.94
2000 QC_{243} (54598)	0.448	Scat	22:39	−06:56	20.6	341.70	1.4 .	19.10
1999 TD_{10} (29981)	0.495[c]	Scat	01:47	+08:05	20.2	30.69	−2.6 .	13.32

[a]Positions for 12/02.
[b] Ecliptic longitude and latitude.
[c](19308) 1996 TO_{66} has circumstantial evidence for activity, and (29981) 1999 TD_{10} has reported coma.

In order to search for faint coma, the images must be combined. Image shifts to compensate for the dithering were computed using the mean difference in the centroids for ∼20 field stars measured in each image. These images were added together and the composite is shown in Figure 2b (the horizontal and vertical streaks at the sides of the images are edge artifacts from the composite). It is clear from the composite that there is significant nebulosity in the background, which makes searching for a low surface brightness coma extremely difficult. A template for the background stars and galaxies was therefore made by creating a background template by median filter combination of all the images from night 1.

The scaled combined template was then subtracted frame by frame from all of the images to remove both the background objects and the nebulosity. The images

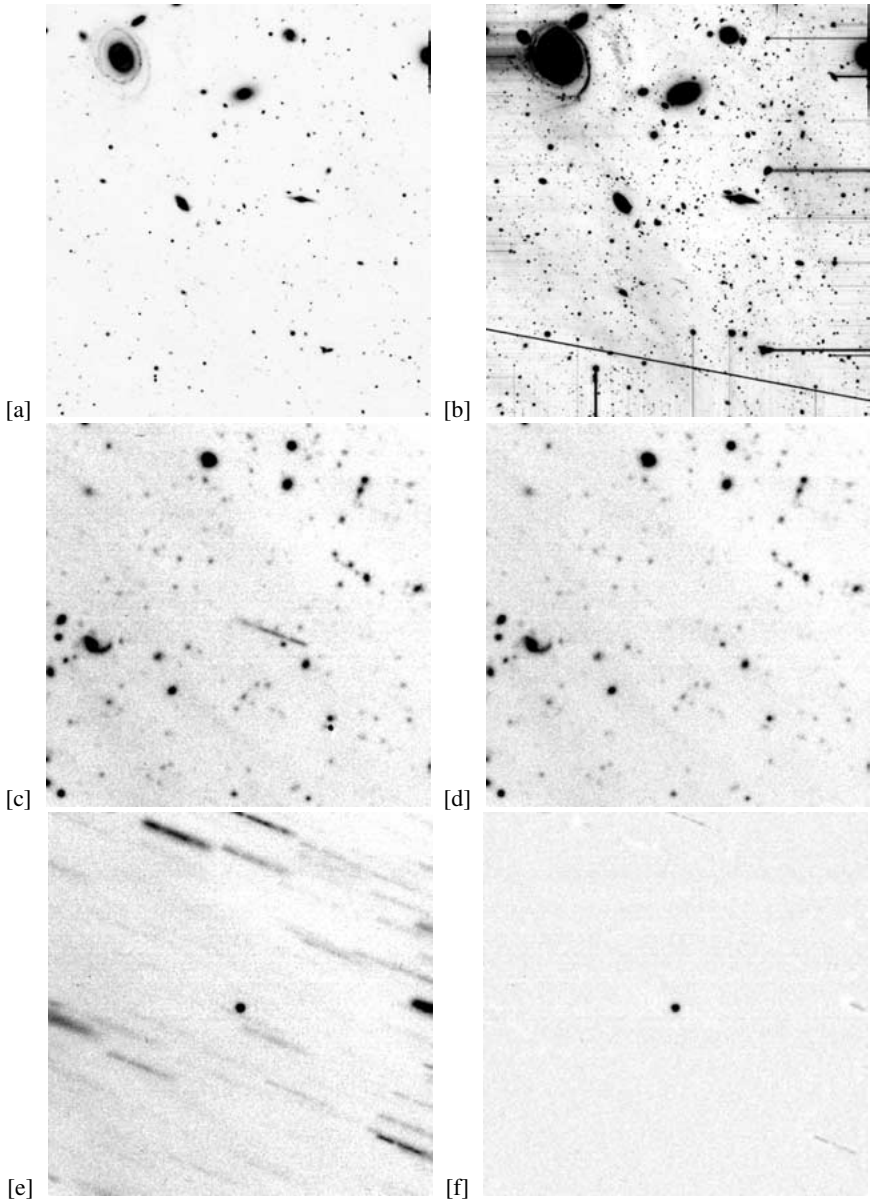

Figure 2. (a) Portion of a single 400 sec V-band image centered on KBO (24952) 1997 QJ_4, 6.3′ on a side; (b) Composite image, 12,400 sec total exposure time; (c) same as (b), but zoomed in for a FOV of 80″. The KBO is the trailed object in the middle; (d) Median combined images to make the star template; (e) Shifted and added image digitally tracked at the KBO rate; (f) Median combined star-galaxy subtracted image showing only the KBO. For all images, N is up and E is left.

TABLE III
KBO (24952) 1997 QJ_4 photometry

JD[a]	UT	χ[b]	$m_V \pm \sigma$	JD[a]	UT	χ[b]	$m_V \pm \sigma$
0.7358	5.6611	1.984	23.339 ± 0.050	0.8896	9.3503	1.029	23.156 ± 0.035
0.7485	5.9631	1.766	23.302 ± 0.046	0.8950	9.4772	1.027	23.222 ± 0.033
0.7537	6.0897	1.690	23.265 ± 0.041	0.9004	9.6131	1.026	23.260 ± 0.034
0.7590	6.2167	1.622	23.249 ± 0.041	0.9058	9.7400	1.026	23.204 ± 0.034
0.7644	6.3436	1.561	23.257 ± 0.039	0.9111	9.8669	1.027	23.268 ± 0.036
0.7732	6.5561	1.471	23.350 ± 0.042	0.9165	9.9939	1.029	23.270 ± 0.037
0.7786	6.6831	1.424	23.193 ± 0.035	1.7861	6.8656	1.345	23.405 ± 0.127
0.7883	6.9192	1.349	23.286 ± 0.037	1.7942	7.0611	1.292	23.012 ± 0.077
0.7937	7.0467	1.313	23.205 ± 0.033	1.7996	7.1881	1.261	23.043 ± 0.147
0.7988	7.1736	1.281	23.098 ± 0.030	1.8101	7.4419	1.208	23.126 ± 0.046
0.8042	7.3003	1.251	23.168 ± 0.033	1.8154	7.5689	1.184	23.268 ± 0.057
0.8096	7.4272	1.224	23.088 ± 0.031	1.8208	7.6958	1.163	23.096 ± 0.049
0.8147	7.5542	1.199	23.101 ± 0.032	1.8259	7.8228	1.143	23.084 ± 0.039
0.8201	7.6811	1.176	23.057 ± 0.031	1.8328	7.9836	1.122	23.176 ± 0.077
0.8252	7.8081	1.156	23.110 ± 0.031	1.8379	8.1106	1.107	23.283 ± 0.057
0.8306	7.9350	1.137	23.003 ± 0.029	1.8433	8.2375	1.093	23.174 ± 0.060
0.8359	8.0619	1.120	23.113 ± 0.032	1.8538	8.4914	1.069	23.134 ± 0.048
0.8413	8.1889	1.105	23.118 ± 0.030	1.8591	8.6183	1.060	23.231 ± 0.067
0.8464	8.3167	1.091	23.128 ± 0.032	1.8645	8.7453	1.051	23.143 ± 0.053
0.8518	8.4436	1.079	23.041 ± 0.030	1.8750	8.9997	1.038	23.076 ± 0.066
0.8572	8.5706	1.068	23.075 ± 0.030	1.8804	9.1267	1.034	23.255 ± 0.098
0.8684	8.8425	1.050	23.095 ± 0.034	1.9014	9.6342	1.026	22.955 ± 0.114
0.8738	8.9694	1.043	23.094 ± 0.033	1.9067	9.7611	1.026	23.198 ± 0.083
0.8789	9.0964	1.037	23.170 ± 0.034	1.9172	10.0150	1.031	23.276 ± 0.104
0.8843	9.2233	1.033	23.175 ± 0.034				

[a] JD-2452550.
[b] Airmass.

were then shifted using the rates of motion as determined from the ephemeris ($d\alpha/dt = -0.0009109$ arcsec s^{-1} and $d\delta/dt = -0.0003611$ arcsec s^{-1}) and the plate scale, and then median combined to make the final composite KBO image shown in Figure 2f.

3.1. Rotational light curve

Photometry was done using the digiphot:apphot package in IRAF, through multiple apertures, although the $1.5''$ radius aperture yielded the best S/N with minimal flux loss. A curve of growth on a standard star showed that 99.5% of the light was

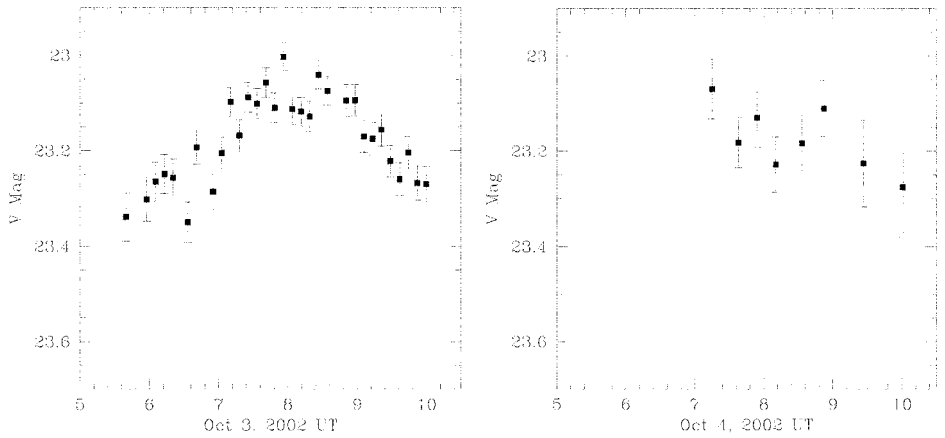

Figure 3. Rotational lightcurve of KBO 24529 on 2002 Oct. 3 and 4 UT. Data on Oct. 4 were taken under very non-photometric conditions, but have been calibrated using differential photometry from the field stars measured on the first night. Only those data with errors < 0.1 mag have been shown.

contained within an aperture of 3.5″ radius, and that for an aperture of 1.5″ radius, there was a light loss of ∼4%. Measurements were made on ∼20 field stars in addition to the KBO, and differential photometry performed, as a check on night 1 and to correct for extinction by cirrus on night 2. The photometry is presented in Table III. All of the data represent 400 sec exposures through the V filter. The 5-σ limiting magnitude for point sources on the composite image was found to be m_V = 30.5.

A plot of the data is shown in Figure 3. A brightness modulation with a range Δm > 0.3 mag is clearly visible. Because we didn't sample enough of the light curve a formal period search is not useful, however it is clear that the rotation period is > 4 hr.

3.2. COMA SEARCH

The most sensitive imaging constraints on mass loss come from a comparison of azimuthally averaged surface brightness profiles of the object in comparison to field stars (Meech and Weaver, 1995). An azimuthally averaged radial surface brightness profile was computed for both the KBO and each of 5 field stars of comparable brightness. The field star fluxes were normalized and averaged at each radial distance to form an average stellar profile for comparison with the surface brightness profile of KBO 24529. Both profiles are shown in Figure 4. There was no coma apparent in either the composite median combined image or in a difference between the surface brightness profiles.

For an untrailed asteroidal object with no coma, the subtraction of the normalized stellar profile fluxes from those of the asteroid should yield a value of zero with an associated error. One can use 3σ of this error as the limiting possible

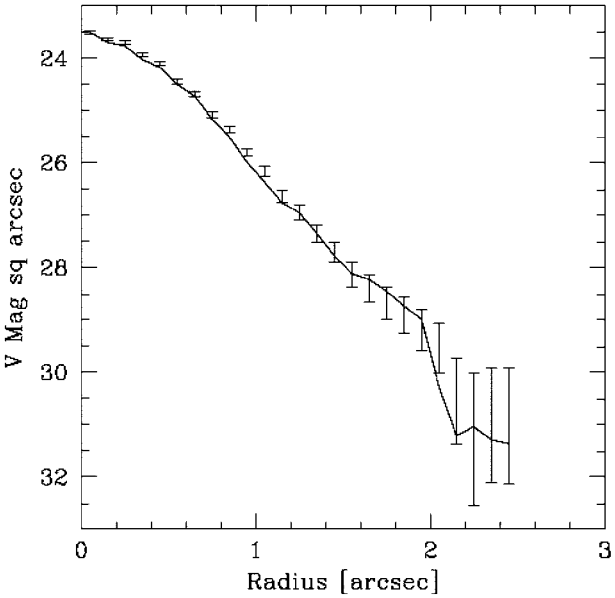

Figure 4. Surface brightness profile of (24529) 1997 QJ_4 (error bars), compared with the normalized average star surface brightness profile (solid line), from the 12,400s composites.

maximum flux contributed from scattered coma light. This flux will be given by (see Appendix 1 for derivation):

$$F = S_{\odot} \pi a_{\rm gr}^2 p_v Q_p \phi / 2 r^2 \Delta^2 v_{\rm gr}, \tag{1}$$

where $S_{\odot}$ is the solar flux through the bandpass [W m^{-2}], $a_{\rm gr}$ [m] the grain radius, $p_{\rm v}$ the grain albedo, Q_p [s^{-1}] the dust production rate, ϕ the projected diameter of the aperture [m], $v_{\rm gr}$ [m s^{-1}] the grain velocity, and r is in AU and Δ in m. If one assumes a Bobrovnikoff relation for the terminal grain velocities, $v_{\rm gr} = v_{\rm bob} = (\mu/\mu_{\rm H_2O})^{0.5} 600\ r^{-0.5}$, and recalls that $\phi = \Delta\phi'/206265$ where ϕ' is the angular size of the aperture in arcsec, then for a given observed flux the dust production will vary as

$$Q_p \propto r^{1.5} \Delta^1 \tag{2}$$

which shows that the most sensitive limits are placed for those objects closest to the Earth and Sun. The total dust production, Q [kg s^{-1}] is obtained from Q_p by multiplying by the grain mass, $m_{\rm gr} = 4/3\ \pi\ a_{\rm gr}^3\ \rho$ (assuming $\rho = 10^3$ kg m^{-3}). The dust limit of 0.01 kg s^{-1} obtained at a distance of 1″ from the core (limited by seeing) for KBO (24952) 1997 QJ_4 is extremely sensitive. It indicates that for sublimation of CO ice, for example, that given a radius of 120 km (for H=7.5, and assuming p_v=0.05), implies a fractional active area of 10^{-8} or 2×10^3 m^2.

3.3. FUTURE WORK

We are in the process of analyzing the data from the whole mosaic to determine the cumulative luminosity functions down to faint levels and verify the break in the slope seen by (Kinoshita et al., 2004). Once other KBOs are identified in the field, deep searches for activity will be conducted for each of the candidates.

4. Appendix 1

The number of grains, n_o, along the line of site centered on the nucleus out to a distance ϕ[m], for a steady state isotropic output is given by:

$$n_o = \frac{\pi Q \phi}{2 v_{\rm gr}} \tag{3}$$

which is obtained by integrating the column density $N(p) = Q/4vp$ in circular annuli centered on the radius, where p is the impact parameter, and $v_{\rm gr}$ is the grain velocity. The volume emission rate from any point in the coma, j, is the product of the incident flux, the grain cross section, the bond albedo and the dust number density, n_o [m^{-3}]:

$$j = \frac{S_\odot}{r^2}(\pi a_{\rm gr}^2) 4 p_v n_o, \tag{4}$$

where r is the heliocentric distance, a_{gr} the grain radius, and p_v the geometric albedo. For isotropic scatterers, the bond albedo, A_B, which is the ratio of the total scattered radiation to the total incident radiation, is $A_B = 4p_v$. For optically thin conditions, the specific intensity, I, is given by:

$$I = \frac{S_\odot (\pi a_{\rm gr}^2) 4 p_v N}{4\pi r^2}, \tag{5}$$

where $N = n_o/(\pi\ \phi^2)$ is the column density [m^{-2}]. The flux is then given by $I \times \Omega$, where Ω is the solid angle of the field of view, $\Omega = \pi\ \phi^2\ /\ \Delta^2$. Thus the flux, F, is

$$F = S_\odot \pi a_{\rm gr}^2 p_v Q_p \phi / 2 r^2 \Delta^2 v_{\rm gr} \tag{6}$$

which is the same as Equation (1).

Acknowledgements

We would like to thank Dr Yutaka Komiyama, the Suprime-Cam instrument support scientist for all his help with the observations. Image processing in this paper

has been performed using the IRAF program. IRAF is distributed by the National Optical Astronomy Observatories, which is operated by the Association of Universities for Research in Astronomy, Inc. (AURA) under cooperative agreement with the National Science Foundation. Support for this work was provided by NASA Grant No. NAG5-12236.

References

Bauer, J. M., Fernandez, Y. R., and Meech, K. J.: 2003, 'An Optical Survey of the Active Centaur C/NEAT (2001 T4)', *Pub. Astron. Soc. Pac.* **115**, 981–989.

Bockelée-Morvan, Lellouch, E., Biver, N., Paubert, G., Bauer, J., Colum, P., and Lis, D. C.: 2001, 'Search for CO Gas in Pluto, Centaurs and Kuiper Belt Objects at Radio Wavelengths', *Astron. Astrophys.* **377**, 343–353.

Boehnhardt, H., Tozzi, G. P., Birkle, K., Hainaut, O., Sekiguchi, T., Vair, M., Watanabe, J., Rupprecht, G., and the FORS Instrument Team: 2001, 'Visible and Near-IR Observations of Transneptunian Objects. Results from ESO and Calar Alto Telescopes', *Astron. Astrophys.* **378**, 653–667.

Boehnhardt, H., Delsanti, A., Barucci, A., Hainaut, O., Doressoundiram, A., Lazzarin, M., Barrera, L., de Bergh, C., Birkle, K., Dotto, E., Meech, K., Ortiz, J. E., Romon, J., Sekiguchi, T., Thomas, N., Tozzi, G. P., Watanabe, J., and West, R. M.: 2002, 'ESO Large Program on Physical Studies of Transneptunian Objects and Centaurs: Visible Photometry – First Results', *Astron. Astrophys.* **395**, 297–303.

Brown, M. E., Blake, G. A., and Kessler, J. E.: 2000, 'Near-Infrared Spectroscopy of the Bright Kuiper Belt Object 2000 EB_{173}', *Astrophys. J.* **543**, L163–L165.

Brown, R. H., Cruikshank, D. P., and Pendleton, Y.: 1999, 'Water Ice on Kuiper Belt Object 1996 TO_{66}', *Astrophys. J.* **519**, L101–L104.

Brown, R. H., Cruikshank, D. P., Pendleton, Y. J., and Veeder, G. J.: 1997, 'Surface Composition of Kuiper Belt Object 1993 SC', *Science* **276**, 937–939.

Brunini, A. and Melita, M. D.: 2002, 'The Existence of a Planet beyond 50 AU and the Orbital Distribution of the Classical Edgeworth–Kuiper Belt Objects', *Icarus* **160**, 32–43.

Bus, S. J., A'Hearn, M. F., Schleicher, D. G., and Bowell, E.: 1991, 'Detection of CN Emission from (2060) Chiron', *Science* **251**, 774–777.

Choi, Y. J., Prialnik, D., and Brosch, N.: 2003, 'Rotation and Cometary Activity of KBO 1999 TD_{10}', *Icarus* **165**, 101–111.

Delsanti, A. C., Boehnhardt, H., Barerra, L., Meech, K. J., Sekiguchi, T., and Hainaut, O. R.: 2001, 'BVRI Photometry of 27 Kuiper Belt Objects with ESO/Very Large Telescope', *Astron. Astrophys* **380**, 347–358.

Doressoundiram, A., Peixinho, N., de Bergh, C., Fornasier, S., Thébault, P., Barucci, M. A., Veillet, C.: 2002, 'The Color Distribution in the Edgeworth–Kuiper Belt', *Astron. J.* **124**, 2279–2296.

Doressoundiram, A., Tozzi, G. P., Barucci, M. A., Boehnhardt, H., Fornasier, S., and Romon, J.: 2003, 'ESO Large Programme on Trans-Neptunian Objects and Centaurs: Spectroscopic Investigation of Centaur 2001 BL_{41} and TNOs (26181) 1996 GQ_{21} and (26375) 1999 DE_9', *Astron. J.* **125**, 2721–2727.

Dotto, E., Barucci, M. A., Boehnhardt, H., Romon, J., Doressoundiram, A., Peixinho, N., de Bergh, C., and Lazzarin, M.: 2003, 'Searching for Water Ice on 47171 1999 TC_{36}, 1998 SG_{35}, and 2000 QC_{243}: ESO Large Program on TNOs and Centaurs', *Icarus*, in press.

Gil-Hutton, R.: 2002, 'Color Diversity Among Kuiper Belt Objects: The Collisional Resurfacing Model Revisited', *Plan. and Space Sci* **50**, 57–62.

Gomes, R. S.: 2003, 'The Origin of the Kuiper Belt High-Inclination Population', *Icarus* **161**, 404–418.

Hahn, J.: 2000, 'The Outer Edge of the Kuiper Belt', *LPSC Conf.* **1797**.
Hainaut, O. R. and Delsanti, A.: 2002, 'Colors of Minor Bodies in the Outer Solar System. A Statistical Analysis', *Astron. Astrophys.* **389**, 641–664.
Hainaut, O. R., Delahodde, C. E., Boehnhardt, H., Dotto, E., Barucci, M. A., Meech, K. J., Bauer, J. M., West, R. M., and Doressoundiram, A.: 2000, 'Physical Properties of TNO 1996 TO_{66}', *Astron. Astrophys.* **356**, 1076–1088.
Jewitt, D. and Luu, J.: 2001, 'Colors and Spectra of Kuiper Belt Objects', *Astron. J.* **122**, 2099–2114.
Kinoshita, D. et al.: 2004, 'Deep KBO Survey Near the Invariable Plane' (this volume).
Kobayashi, H. and Ida, S.: 2001, 'The Effects of a Stellar Encounter on a Planetesimal Disk', *Icarus* **153**, 416–429.
Landolt, A.: 1992, 'UBVRI Photometric Standard Stars in the Magnitude Range $11.5 < V < 16.0$ Around the Celestial Equator', *Astron. J.* **104**, 340–371.
Licandro, J., Oliva, E., and Di Martino, M.: 2001, 'NICS-TNG Infrared Spectroscopy of Trans-Neptunian Objects 2000 EB_{173} and 2000 WR_{106}', *Astron. Astrophys.* **373**, L29–L32.
Licandro, J., Ghinassi, F., and Testi, L.: 2002, 'Infrared Spectroscopy of the Largest Known Trans-Neptunian Object 2001 KX_{76}', *Astron. Astrophys.* **388**, L9–L12.
Luu, J. X. and Jewitt, D. C.: 1998, 'Optical and Infrared Reflectance Spectrum of Kuiper Belt Object 1996 TL_{66}', *Astrophys. J.* **494**, L117.
Luu, J. X., Jewitt, D. C., and Trujillo, C.: 2000, 'Water Ice in 2060 Chiron and Its Implications for Centaurs and Kuiper Belt Objects', *Astrophys. J.* **531**, L151–L154.
Meech, K. J.: 1999, 'Chemical and Physical Aging of Comets', in J. Svoreň, E. M. Pittich and H. Rickman (eds.), *Evolution and Source Regions of Asteroids and Comets*, Publisher: IAU Colloq. 73, Astron. Inst. Slovak Acad. Sci., pp. 195–210.
Meech, K. J. and Belton, M. J. S.: 1990, 'The Atmosphere of 2060 Chiron', *Astron. J.* **100**, 1323–1339.
Meech, K. J. and J. Svoreň, J.: 2004, 'Using Cometary Activity to Trace the Physical and Chemical Evolution of Cometary Nuclei', in M. Festou et al. (eds.), *CometsII*, University of Arizona Press, Tucson, AZ, in press.
Meech, K. J. and H. A. Weaver, H. A.: 1995, 'Unusual Comets (?) as Observed from the Hubble Space Telescope', *Earth, Moon and Planets*, **72**, 119–132.
Miyazaki, S., Sekiguchi, M., Imi, K., Okada, N., Nakata, F., and Komiyama, Y.: 1998, 'Characterization and Mosaicking of CCDs and the Applications to the Subaru Wide-Field Camera (Suprime-Cam)', in S. D'Odorico (ed.), *Proc. SPIE 3355: Optical Astronomical Instrumentation*, p. 363.
Prialnik, D., Brosch, N., and Ianovici, D.: 1995, 'Modelling the Activity of 2060 Chiron', *MNRAS* **276**, 1148–1154.
Sekiguchi, T., Boehnhardt, H., Hainaut, O. R., and Delahodde, C. E.: 2002, 'Bicolour Lightcurve of TNO 1996 TO_{66} with the ESO-VLT', *Astron. Astrophys.* **385**, 281–288.
Stern, S. A.: 2001, 'Evidence for a Collisional Mechanism Affecting Kuiper Belt Object Colors', *Astron. J.* **124**, 2297–2200.
Trujillo, C. A. and Brown, M. E.: 2002, 'A Correlation between Inclination and Color in the Classical Kuiper Belt', *Astrophys. J.* **566**, L125–L128.
Weidenschilling, S. J.: 2003, 'Planetesimal Formation in Two Dimensions: Putting an Edge on the Solar System', *LPSC* **1707**.
West, R. M., Hainaut, O. R., and Smette, A.: 1991, 'Post-Perihelion Observations of Comet P/Halley III: An Outburst at R = 14.3AU', *Astron. Astrophys.* **246**, L77–L81.
Womack, M. and Stern, S. A.: 1999, 'The Detection of Carbon Monoxide Gas Emission in (2060) Chiron', *Astronomicheskii Vestnik* **33**, 1987.